ELSEVIER

Catalysis Today 35 (1997) 247–268

CATALYSIS TODAY

Mechanisms of phase separation in gel-based synthesis of multicomponent metal oxides

Y. Narendar, Gary L. Messing

Department of Materials Science and Engineering, The Pennsylvania State University, University Park, PA 16802, USA

Abstract

The principles underlying metal oxide phase formation from multicomponent molecular gels are reviewed. The critical phase separation mechanisms operating at each stage of the gel process, viz. gel synthesis, gel thermolysis and oxide crystallization, are described with examples from the synthesis literature on aluminosilicates, cuprates and lead-based perovskites. It is demonstrated that direct crystallization of the equilibrium metal oxide requires synthesizing a cation-homogeneous gel, avoiding phase separation during thermolysis, and providing a low energy barrier for nucleation of the equilibrium phase. The influence of synthesis parameters and heating conditions on chemical phase separation are explained and guidelines for regulating the direct formation of metal oxides are outlined.

1. Introduction

Sol-gel processing is one of the most effective techniques for synthesizing multicomponent oxides which are difficult to prepare by conventional ceramic processing. Several sol-gel techniques have been developed for multicomponent metal oxide preparation including alkoxide hydrolysis, particulate gels and metal carboxylates such as citrate gels. Particulate gels are composed of aggregated colloidal particles dispersed on the scale of tens or hundreds of nanometers. In this paper the discussion is restricted to alkoxide and carboxylate gel precursors, which have the potential of cation mixing at the molecular scale and thus the potential for direct crystallization of multicomponent oxides.

Alkoxide based gels (or powders) are obtained by hydrolyzing molecular precursors such as mixtures of metal alkoxides or metal alkoxides and metal salts into an oxide (or hydroxide) network via inorganic polymerization reactions. Amorphous metal carboxylate gels are synthesized by crosslinking a concentrated solution of carboxylato-metal complexes into a three dimensional gel structure with ammonium carboxylate, metal carboxylate, ester or hydrogen bonds. In gel-based synthesis the cations are molecularly mixed and spatially fixed in the gel, reducing diffusion distances during thermolysis and thus lowering the temperature for oxide formation.

Achieving a homogeneous cation distribution is critical to realizing the advantages of sol-gel processing. While sol-gel processing has the potential for cation mixing at the molecular scale, it is usually observed that gels do not directly crystallize into the desired or equilib-

PII S0920-5861(96)00160-5

rium oxide phase [1–4]. The formation of reaction intermediates necessitates a high temperature solid state reaction to form phase pure systems and compromises the advantages of the sol-gel process. The formation of intermediates is evidence that chemical phase separation is quite common in multicomponent gels. Cation segregation is observed in TEM micrographs of multicomponent gels. Hsueh and Mecartney demonstrated by TEM that acid-catalyzed lead zirconate titanate (PZT) gels have an inhomogeneous Zr distribution in films during the initial stage of heating [5]. Similarly, Huling and Messing observed an interpenetrating structure of Al-rich and Si-rich regions separated at the scale of ca. 5 nm in TEM micrographs of amorphous mullite gels prepared from $Al(NO_3)_3 \cdot 9H_2O$ and $Si(OEt)_4$ and heated to 900°C [6].

Chemical phase separation is determined by the thermodynamic driving force and the kinetics of ionic diffusion. Due to high temperatures (> two thirds of the melting temperature) employed in melt forming or conventional materials processing, mobility is high and phase separation is determined by thermodynamics. In glasses (or metals), a large positive enthalpy of mixing in systems such as alkaline earth metal silicates or aluminosilicates leads to phase separation in the liquid or during cooling to form a glass [7,8]. In polymer solutions, the entropy of mixing is small and the positive mixing enthalpy causes phase separation [9]. Phase separation during gel processing is essentially determined by kinetic factors because oxide formation from gels occurs at low temperatures where long range diffusion, necessary for phase separation, is kinetically hindered. The formation of solid solutions in systems with limited phase miscibility, such as ZrO_2–metal oxides [10] and homogeneous glass compositions within the immiscibility gap of alkaline earth silicates systems [11,12], are examples of kinetically-limited formation of oxides from gels.

Hence, it is important to obtain a homogeneous cation distribution in the gel and maintain the cation homogeneity during the thermal treatment to convert the gel into a crystalline oxide or glass. Recognizing the importance of cation homogeneity, several researchers have concentrated on synthesizing homogeneous multicomponent gels. However, phase separation is not restricted to scale-of-mixing arguments during gel synthesis and even homogeneous gels, such as aluminosilicate gels, are observed to phase separate on heating [6].

The aim of this review is to elucidate mechanisms which can lead to phase separation during oxide formation and to provide guiding principles for direct formation of mixed metal oxides. Most of the fundamental research on alkoxide-derived multicomponent systems, especially that focused on gel structure and cation homogeneity, has been on multicomponent silicates, especially aluminosilicates. Consequently, most of the examples and discussion on alkoxide-derived systems will be based on the literature on mullite ($3Al_2O_3 \cdot 2SiO_2$) [1,13,14] and cordierite ($2MgO \cdot 2Al_2O_3 \cdot 5SiO_2$) [2,15]. In the alumina–silica system the orthorhombic form of mullite (o-mullite) is the stable form of mullite for a Al_2O_3:SiO_2 stoichiometry of 3:2. However, two metastable intermediates are commonly observed at low temperatures on heating alkoxide-derived mullite gels, a tetragonal form of mullite (t-mullite) with the composition $2Al_2O_3 \cdot SiO_2$ and a spinel phase ($6Al_2O_3 \cdot SiO_2$). Because the Al_2O_3:SiO_2 ratio is different in spinel, t-mullite and o-mullite, oxide phase development is a good measure of the cation homogeneity and nucleation conditions in the gel before oxide formation. Thus, sol-gel synthesis of mullite serves as an excellent example of how phase separation can offset crystallization of stable phases from gels.

The carboxylate gel literature is focused on synthesis of materials with perovskite-derived structures such as titanates [16,17], chromates [18] or cuprates [19,20]. Thus, ferroelectric Pb-based perovskites (lead zirconate titanate [21] or lead magnesium niobate [3,22]) and superconducting yttrium barium copper oxide [19] will

serve as the key examples of phase separation in carboxylate gels.

In the first section the effect of different synthesis parameters on gel structure and consequently oxide formation will be addressed. In the second section the effect of thermolysis (viz. heating) on gel structure and its effects on oxide crystallization pathway is discussed. Lastly, the role of nucleation on oxide crystallization will be discussed.

2. Gel synthesis-alkoxide derived gels

Gel synthesis involves polymerizing molecular precursors into a three dimensional network and subsequently converting the wet gel into a xerogel by removing the solvent. The critical step in gel synthesis is to molecularly mix and to spatially fix the individual components before subsequent heating (referred to as gel thermolysis).

Alkoxide-based gels are synthesized from metal alkoxides or mixtures of metal salts and metal alkoxides. The precursors hydrolyze readily in water to form partially hydrolyzed monomers as shown in Eq. (1).

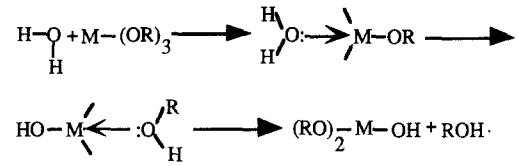

(1)

Partially hydrolyzed monomers condense via alcoxolation (Eq. (2)) and oxolation (Eq. (3)) or olation (Eq. (4)) reactions to form oligomers. The oligomers grow into larger clusters through further condensation reactions and a three dimensional gel network is formed after cluster–cluster impingement. A schematic of gel formation from hydrolyzed alkoxide precursors is shown in Fig. 1 [23].

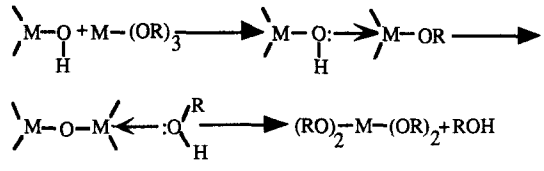

(2)

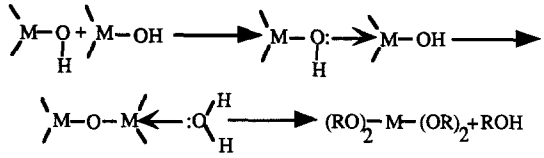

(3)

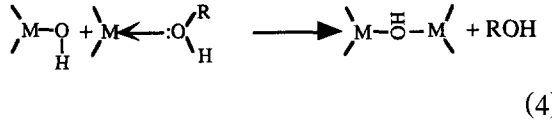

(4)

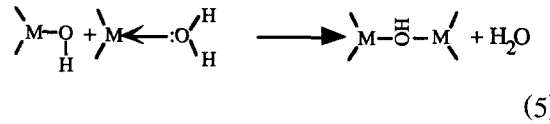

(5)

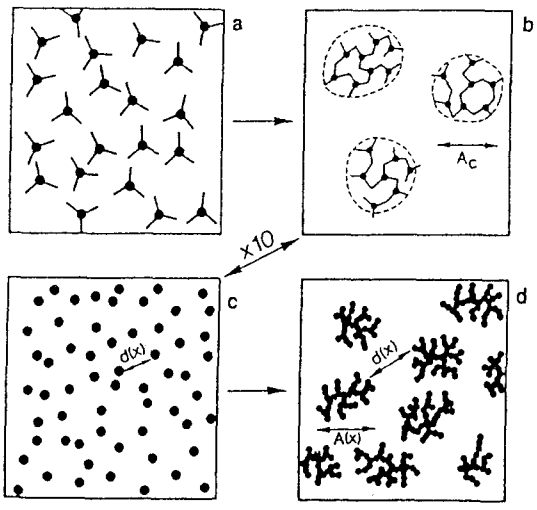

Fig. 1. Schematic of polymerization reactions leading to gels from hydrolyzed alkoxides: (a) precursor monomers in solution, (b) and (c) elementary units resulting from the first condensation reactions and (d) clusters developed by aggregation of elementary units [23].

The hydrolysis rate depends on the electrophilicity of the metal atom and its ability to

undergo coordination expansion [24]. Hence the hydrolysis rates are widely different for different metals, for example Ti hydrolyzes five orders of magnitude faster than Si [24]. The synthesis issues in multicomponent alkoxide gels are primarily related to differences in the hydrolysis and condensation rates of alkoxides of different metals. A large difference in the hydrolysis rates of alkoxides, as seen between Si and Ti alkoxides, favors homocondensation (Ti–O–Ti linkages) over heterocondensation (Ti–O–Si linkages) and leads to segregation of Ti and Si in the gel. Cation segregation leads to crystallization of secondary phases, such as TiO_2 (anatase) from phase separated SiO_2–TiO_2 gels [25].

To form a homogeneous gel from a mixture of alkoxides with different hydrolysis rates, it is critical to separate the hydrolysis and condensation regimes. Decoupling the two reaction regimes allows heterocondensation between the different hydrolyzed alkoxides and reduces the degree of cation segregation as a result of homocondensation reactions. Several approaches are used to separate the hydrolysis and condensation regimes and hence improve the gel homogeneity. These include, lowering the concentration of water for hydrolysis, partial hydrolysis of the slowest reacting species, acid or base catalysis, formation of heterometallic alkoxides and reducing the hydrolysis rate of highly reactive species using chelating agents.

Because hydrolysis is limited by the water concentration in the alkoxide mixture, both the amount of water and the rate of water addition to the alkoxide mixture strongly influence gel homogeneity [26]. Rapid hydrolysis rates due to high water concentration and a rapid rate of water addition are the primary reasons for cation segregation in most gels [1,4,8], especially in mixed metal alkoxide systems with widely different hydrolysis rates. The effects of cation segregation due to high water concentration is illustrated by the work of Hayashi et al. [25] on TiO_2–SiO_2 gels prepared from Ti(*i*-OPr)$_4$ and Si(OEt)$_4$ by hydrolysis with water in the presence of HCl as a catalyst. Gels prepared at low water concentrations (water/alkoxide ratio = 16) were clear, transparent and led to homogeneous TiO_2–SiO_2 glasses on heating to 800°C. However, gels prepared at high water concentration (water/alkoxide molar ratio = 50) were inhomogeneous, opaque and porous. The rapid hydrolysis of Ti(*i*-OPr)$_4$ to form Ti–O–Ti linkages at high water concentrations, results in cation segregation in the gel and heating the phase separated gel to 500°C results in formation of crystalline TiO_2 (anatase).

Apart from a low amount of water, a slow rate of water addition is also critical to avoid cation segregation and form homogeneous gels. Yoldas and Partlow [26] studied the effect of the rate of addition of water on the crystallization behavior of mullite from aluminosilicate gels prepared by hydrolyzing a mixture of Al(sec.-OBu)$_3$ and Si(OEt)$_4$. Gels prepared by slow hydrolysis from atmospheric humidity over a period of 90 days lead to direct t-mullite formation at 980°C accompanied with a sharp exothermic peak in a differential thermal analysis (DTA) scan. However, an exothermic peak in the 1000°C range is absent in gels prepared by directly adding water to the alkoxide mixture. Sen and Thiagarajan [27] synthesized aluminosilicate gels using a procedure similar to Yoldas but observed spinel ($6Al_2O_3 \cdot SiO_2$) formation at 950°C, with o-mullite ($3Al_2O_3 \cdot 2SiO_2$) crystallizing above 1100°C. Spinel formation observed by Sen and Thiagarajan [27] is most likely related to a shorter gelation time of two weeks compared to six weeks used by Yoldas and Partlow [26].

Literature on crystallization from aluminosilicate gels clearly shows that gel formation in the presence of a base catalyst leads to spinel formation before mullite crystallization [1,28–30]. A deleterious effect of base catalysis on mullite formation is observed in aluminosilicate gels prepared from $Al(NO_3)_3 \cdot 9H_2O$ and Si(OEt)$_4$ [29]. Gels prepared without ammonia crystallized t-mullite ($2Al_2O_3 \cdot SiO_2$) on heating to 980°C, while gels prepared in the ammonia

formed spinel ($6Al_2O_3 \cdot SiO_2$) at 1000°C. A comparison of the IR spectra of gels prepared with ammonia to a mixture of colloidal aluminum hydroxide and silica, clearly shows that presence of ammonia leads to the formation of silica-rich and alumina-rich regions in the gel. The cation segregation in basic conditions is related to the condensation of $Si(OEt)_4$ into colloidal sized particles and possibly the polymerization of aluminum ions into amorphous hydrous oxides. Sanz et al. [30] compared gels prepared by hydrolyzing $Si(OEt)_4$ and Al(sec.-$OBu)_3$ in the presence of ammonia and particulate gels made from a mixture of sols of SiO_2 and AlOOH. Spinel formed from both gel types at 1000°C and pure o-mullite formed above 1300°C. Moreover, the ^{27}Al-NMR spectra of the two gels were similar in the temperature range from 400–1200°C (Fig. 2). The similarity of alkoxide-derived and particulate gel indicates that the scale of cation segregation is at the colloidal scale (tens of nm) in alkoxide-derived gels prepared in the presence of ammonia.

The above results clearly show that a slow hydrolysis rate is critical to obtain a homogeneous gel from multicomponent alkoxide solutions. A low water amount, slow water addition or acidic conditions promote hydrolysis of the slowest reacting metal alkoxides (such as Si), before extensive condensation of the fast reacting metal alkoxide (like Al or Ti). Hence, slow hydrolysis conditions decouple the hydrolysis and condensation regimes. Moreover, heterocondensation between the Al and Si or Si and Ti is also possible, leading to the formation of homogeneous gels with little or no cation segre-

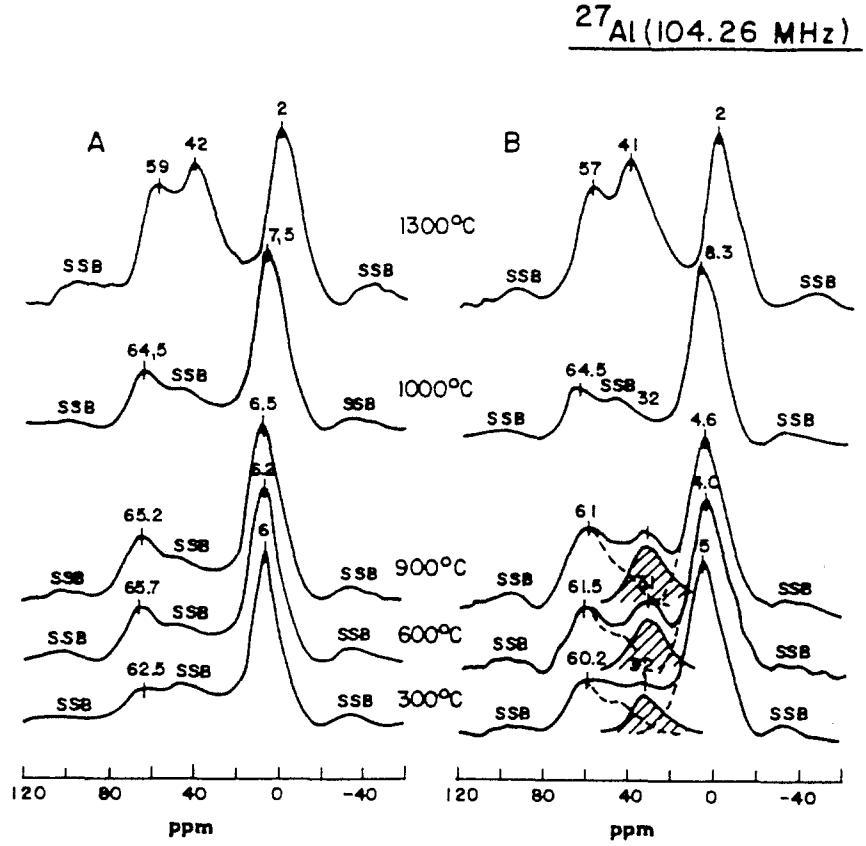

Fig. 2. ^{27}Al-MAS-NMR spectra of (a) base-catalyzed mullite gels and (b) particulate gel of AlOOH and SiO_2, heated to different temperatures. Spinning side-bands are labeled as SSB [30].

gation. However, large amounts of water, rapid addition or base catalysis leads to preferential hydrolysis and homocondensation of the fast reacting species, with little or no heterocondensation. Consequently, rapid hydrolysis results in extensive cation segregation and leads to crystallization of off-stoichiometric intermediates before formation of the desired oxide phase.

While base catalysis leads to inhomogeneous gels in the aluminosilicate system, it is beneficial for obtaining homogeneous gels in the cordierite system. Okuyama et al. [31] observed that base-catalyzed hydrolysis was favorable for forming homogeneous magnesium aluminosilicate gels. Gels formed at pH ca. 1 phase separated even when slowly hydrolyzed with dropwise additions of water and crystallized intermediates such as SiO_2-rich β-quartz$_{(ss)}$ and $MgAl_2O_4$ spinel apart from α-cordierite on heating to 1050°C (Fig. 3). In an intermediate pH range of 3–11, cation homogeneity in gels depended on hydrolysis rate. Slowly hydrolyzed gels formed α-cordierite at 1050°C, while rapid hydrolysis led to extensive phase separation during gelation and the formation of $MgAl_2O_4$ spinel and SiO_2-rich β-quartz$_{(ss)}$ at 1050°C. Cordierite crystallization from base catalyzed magnesium aluminosilicate gels is insensitive to the rate of water addition and gel precipitates obtained with dropwise or rapid addition of alkaline water at pH > 11, both crystallized α-cordierite on heating to 1050°C.

A comparison of the mullite and cordierite crystallization indicates that the formation conditions for homogeneous aluminosilicate and magnesium aluminosilicate gels are different. While extremely slow hydrolysis is required for synthesizing homogeneous aluminosilicate gels, homogeneous magnesium aluminosilicate gels form even under conditions of rapid hydrolysis. The relative insensitivity of the magnesium aluminosilicate gel homogeneity to the synthesis conditions is due to the presence of heterometallic complexes in the alkoxide solution before gelation. Okuyama et al. [31] prepared a mixed alkoxide solution for cordierite by sequentially adding Al(sec.-OBu)$_3$ and Mg metal to prehydrolyzed Si(OEt)$_4$. ^{27}Al-NMR and Raman spec-

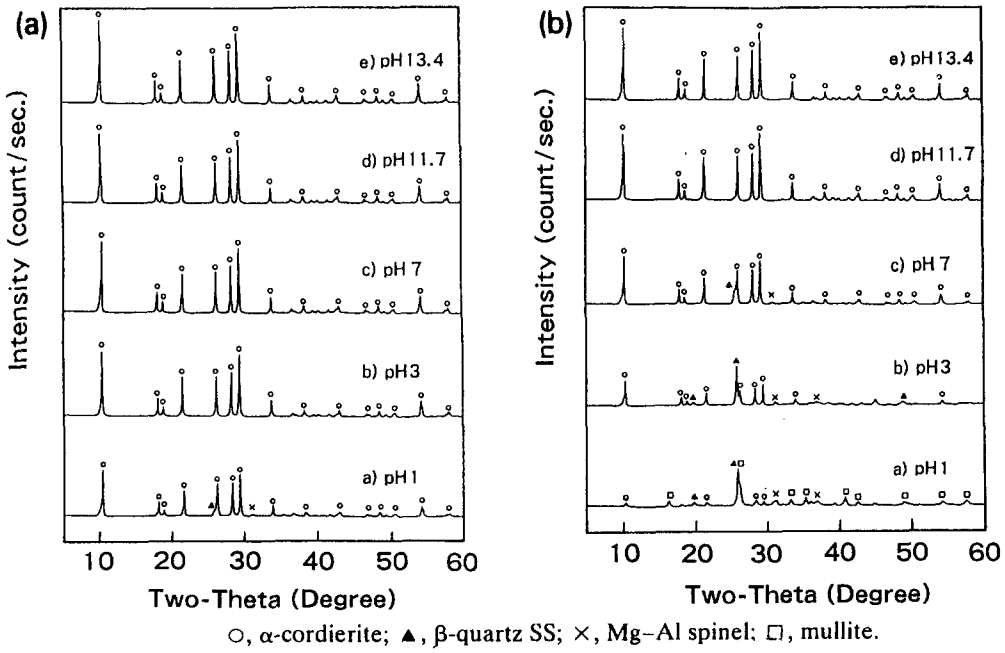

○, α-cordierite; ▲, β-quartz SS; ×, Mg–Al spinel; □, mullite.

Fig. 3. X-ray diffractograms of cordierite gels, prepared by (a) dropwise additions and (b) rapid addition of water with different pH values and heated to 1050°C for 1 h [31].

tra of the alkoxide precursor to cordierite were similar to that of the Mg–Al double alkoxide ($Mg[Al_2(i\text{-}OPr)_8]$) [32], indicating the presence of bimetallic Mg–O–Al in the mixed alkoxide solution. The formation of Al–O–Si linkages in the precursor is evidenced by the considerable broadening of the 4-coordinated resonance peak in ^{27}Al-NMR of the mixed alkoxide solution for cordierite compared to the Mg–Al double alkoxide ($Mg[Al_2(i\text{-}OPr)_8]$). The formation of heterometallic linkages in the cordierite precursor leads to a homogeneous gel with most Al occupying tetrahedral sites, as ascertained by ^{27}Al-NMR. Only under extreme hydrolysis conditions, such as rapid addition of H_2O under acidic condition, are the heterometallic complexes dissociated resulting in phase separation during gelation.

The formation of heterometallic species is observed in several alkoxide systems [33,34], apart from cordierite, and is reported to enhance homogeneity of multicomponent gels [35,36]. Hirano and Kato studied the effect of heterometallic $Li[Nb(OEt)_6]$ formation on $LiNbO_3$ crystallization [37]. A solution of LiOEt and $Nb(OEt)_5$, hydrolyzed immediately after mixing, formed precipitates during gelation. The precipitated gel phase separated to form a Li-rich phase, Li_3NbO_4, and a Nb-rich phase, $LiNb_3O_8$, on heating. On refluxing a solution of LiOEt and $Nb(OEt)_5$ for 24 h and forming $Li[Nb(OEt)_6]$, a clear gel formed after hydrolysis and $LiNbO_3$ directly crystallized at 350°C.

Heterometallic alkoxides eliminate the problem of mismatched hydrolysis rates as each molecule contains the cation mixed in the desired ratio. Consequently, heterometallic alkoxides lead to a uniform cation distribution in the gel. Even the formation of off-stoichiometric heterometallic complexes, with respect to the stoichiometry of the desired oxide, is beneficial as the hydrolysis rates of heterometallic alkoxides is slower than the individual alkoxides [33]. The critical issue in heterometallics is to prevent the dissociation of the complex during hydrolysis [33].

Apart from the several chemical approaches to overcome mismatched hydrolysis rates, physical approaches such as spray pyrolysis are also useful to synthesize homogeneous gels. Spray pyrolysis involves converting a partially hydrolyzed alkoxide precursor into an aerosol and subsequently pyrolyzing the droplets into solid particles by passing the aerosol into a heated furnace. Sakurai et al. [38] prepared a mullite precursor by adding $Al(i\text{-}OPr)_3$ to $Si(OEt)_4$ prehydrolyzed in acidic conditions and refluxing at 75°C for 6 h. The mixed alkoxide solution was sprayed into a furnace maintained between 400 and 600°C. The powder after pyrolysis of the alkoxide solution directly formed t-mullite ($2Al_2O_3 \cdot SiO_2$) after heating to 990°C. Suzuki and Saito [39] synthesized aluminosilicate gels using a similar procedure to Sakurai et al., but did not use spray pyrolysis to form the gel precursor. Suzuki and Saito observed spinel ($6Al_2O_3 \cdot SiO_2$) crystallization at 990°C and o-mullite ($3Al_2O_3 \cdot 2SiO_2$) formed above 1200°C. A similar beneficial effect of spray pyrolysis is also observed in aluminosilicate gels synthesized from $Al(NO_3)_3 \cdot 9H_2O$ and $Si(OEt)_4$. Kanzaki et al. [40] spray pyrolyzed a stoichiometric mixture of $Si(OEt)_4$ and $Al(NO_3)_3 \cdot 9H_2O$ and observed direct t-mullite formation at 970°C. During spray pyrolysis, the residence time of the droplet in the furnace is short (< 10 s) and the rate of solvent removal is expected to be faster than the rate of polymerization reactions between the prehydrolyzed Al and Si species. Consequently, cation segregation during gelation, aging and drying, inherent to conventionally prepared gels, is avoided. A homogeneous Al and Si cation distribution in the solution stage of the alkoxide process is maintained in the solid particles after spray pyrolysis, leading to direct t-mullite formation.

3. Gel synthesis — carboxylates

In carboxylate gels, the metal cations react with carboxylate ligands to form carboxylate

complexes. The structure of the carboxylate complex depends on the nature of the ligand, pH and temperature. The classical chelation mechanism consists of a succession of deprotonation (Eq. (6)), complexation and polymerization reactions (Eq. (7)), as described by Baes and Mesmer [41].

$$[M(H_2O)n]^{z+} \rightarrow [M(OH)_m(H_2O)_{n-m}]^{+(z-m)} + mH^+ \quad (6)$$

$$x[M(H_2O)_n]^{z+} + yOH^- + aA^- \rightarrow [M_xO_u(OH)_{y-2u}A_a]^{(xz-y-a)+} + (xn + u - n)H_2O \quad (7)$$

On concentrating a solution of metal carboxylate complexes, viscosity rises above a critical metal concentration. The high viscosity prevents precipitation of metal carboxylate complexes and on further dehydration a clear gel forms. On cooling the viscous dehydrated gel undergoes a rubber to glass transition and converts to a brittle polymer glass. Based on the moisture sensitivity of carboxylate gels and IR structural studies on carboxylate gels, it is apparent that crosslinks between metal carboxylate complexes are ionic metal carboxylate or ammonium carboxylate bonds [42]. Gels with H-bonds serving as primary crosslinks are also reported [43].

An anionic bridging mechanism, similar to carboxylate ligands, is also observed for precipitates involving HSO_4^- or $H_2PO_4^-$ which form strong coordination complexes with metal cations [44]. Similar ionic metal-carboxylate bonds are documented in the ionomer literature [45] and are also responsible for crosslinking organic dibasic acids such as sebacic acid ($HOOC-(CH_2)_{20}-COOH$) into polymer-like structures [46]. Consequently, metal carboxylate gels which consist of a network of carboxylate complexes and ammonium ions [43] are expected to have a structure similar to crystalline metal citrate precipitates such as $K_2[Ni(C_6H_5O_7)(H_2O)_2]_2 \cdot 4H_2O$ [47]. A schematic of the metal carboxylate gel structure is shown in Fig. 4 [47]. The amorphous nature of the gels could be due to a number of factors

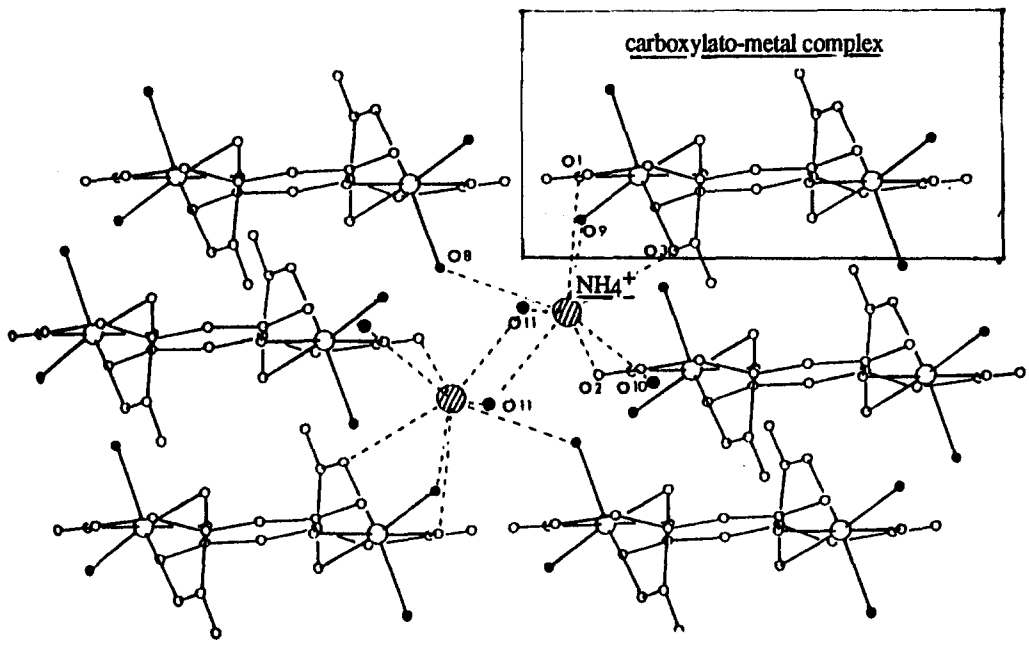

Fig. 4. Schematic of the structure of a metal carboxylate gel, showing metal carboxylate complexes bridged by ionic ammonium (NH_4^+)–oxygen(O) bonds into a three dimensional structure [47].

including, the high viscosity of the solution preventing long range ordering, steric hindrance due to the bulky nature of the complexes and random three dimensional crosslinking. A variation of the carboxylate gel process is the Pechini process [17], where ethylene glycol is used as the solvent for the metal carboxylate complexes. In the Pechini process, ethylene glycol and metal carboxylate complexes react to form esters and consequently, the degree of crosslinking between the carboxylato-metal complexes is increased with both ester bonds and metal carboxylate bridges in the gel.

Because metal carboxylate complexes are the basic structural units in carboxylate gels, the key synthesis issue is the formation of the carboxylato-metal complexes. The formation reaction of a simple metal complex (ML) is shown in Eq. (8),

$$M^{z+} + L^{y-} \rightarrow ML^{-(y-z)} \quad (8)$$

The equilibrium constant for the ML formation reaction is given by the expression $K = [M][L]/[ML]$ and the amount of complex formed is proportional to the ligand concentration $[L]$ and the formation constant K. Thus, excess chelating agent is usually required to ensure a low free metal ion concentration in the solution. The amount of excess chelating agent required depends on the formation constant of the carboxylato-metal constant. Complexes with a large formation constant are preferred as they require a lower concentration of chelating agent.

Since the type of complex is also determined by the pH, the pH, ligand and cation concentration have to be controlled to form carboxylato-metal complexes with all the cations to form a metal carboxylate precursor solution. Incomplete cation chelation leads to selective precipitation of the metal salts (nitrates) or hydroxides of the uncomplexed cations during dehydration, as observed in the synthesis of Y–Ba–Cu-citrate gels.

Chu and Dunn [48] prepared citrate precursors to yttrium barium copper oxide by reacting a mixed solution of yttrium, barium and copper nitrate with citric acid. On dehydrating the mixed cation solution, $Ba(NO_3)_2$ precipitated from the solution. However, on increasing the pH to 6 with NH_4OH, precipitation did not occur and an amorphous gel precursor formed. The precipitation of $Ba(NO_3)_2$ at low pH indicates incomplete complexation of Ba^{2+} with citric acid. Their results are consistent with the effect of pH on the formation constant of alkaline earth metal-citrate complexes [49]. At acidic pH, BaH_2Cit^+ is the predominant species in the solution. However, because the formation constant of BaH_2Cit^+ is small ($\log K = 0.6$), the majority of the Ba^{2+} ions are not complexed with citric acid and $Ba(NO_3)_2$ precipitates. At neutral pH, $BaCit^-$ is the predominate species with a higher formation constant ($\log K = 2.95$). Hence, most of the Ba^{2+} ions are fully complexed and amorphous gels form. However, $Ba(NO_3)_2$ also precipitated from clear gels formed at pH 6 on heating to 200°C, implying the presence of uncomplexed Ba^{2+}. Since $BaCit^-$ formation is influenced by both pH and citric acid concentration, the presence of unchelated Ba^{2+} is indicative of a lower citric acid concentration. The precipitation problem in Y–Ba–Cu-citrate gels was circumvented by Karen and Kjekshus [50], by using a citric acid to metal ratios in excess of the stoichiometry of the carboxylato-metal complex.

Apart from issues of precipitation due to insufficient chelation, precipitation of carboxylato-metal complexes during dehydration was observed in our work and was also reported by Karen and Kjekshus [50]. Metal carboxylate precipitation is controlled by several factors including the pH, structure of the metal carboxylate complex and, most importantly, viscosity of the mixed carboxylate solution and synthesis procedure. For example in our work on Pb–Mg–Nb-citrate gels, an alkaline pH ca. 9.5–10 and excess citric acid (Pb:citric acid molar ratio = 1:4) were required to prevent Pb_3Cit_2 precipitation during the dehydration process. In the Pb-citrate system, several different citrato-metal complexes are formed depending on the pH

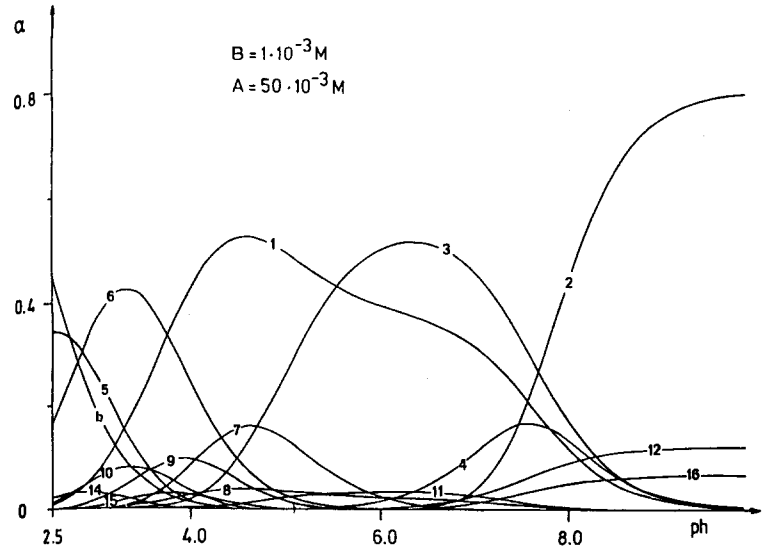

Fig. 5. The relative amounts (α) of the lead citrate complexes as function of pH [51]. A = total mol of citric acid, B = total mol of Pb^{2+}, 1: $PbCit^-$, 2: $Pb_2Cit_2^{4-}$, 3: $PbCit_2^{4-}$, 4: $Pb_2Cit_2^{3-}$, 5: PbH_2Cit^+, 6: $PbHCit^0$, 7: $Pb(HCit)Cit^{3-}$, 9: $PbHCit_2^{3-}$, 12: $PbCit^{2-}$, 16: $Pb_2Cit_2^{6-}$.

range [51]. The speciation curves of the different citrato-lead complexes as a function of pH are shown in Fig. 5 [51]. PbH_2Cit^+, $PbHCit^0$ and $PbCit^-$ form in the acidic range while $PbCit^{2-}$, $PbCit_2^{4-}$ form in the neutral to alkaline range and $PbCit_2^-$ and $Pb_2Cit_2^{4-}$ form in the alkaline range. In the pH range between 2.5 and 7.5 $PbCit^{2-}$ or $PbCit^-$ combine with lead cations to form precipitates $Pb[PbCit^-]_2$ or $Pb_2[PbCit_2^{4-}]$ with the Pb_3Cit_2 stoichiometry [52]. $Pb_2Cit_2^{4-}$ complexes are the predominant species above pH 9 and are stable in the presence of excess citric acid. Consequently, Pb–Mg–Nb-citrate gels formed in alkaline conditions with excess citric acid are homogeneous. Selective precipitation of metal carboxylates

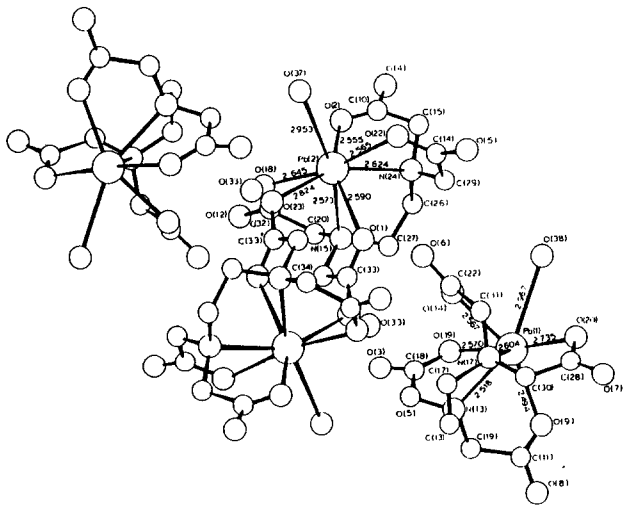

Monomeric and dimeric EDTA-Pb

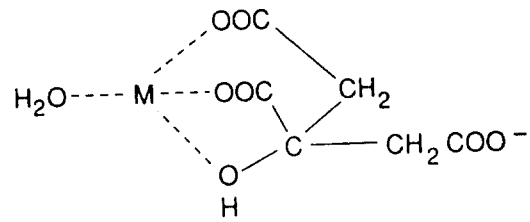

Monomeric citrato-Pb

Fig. 6. Structure of aqueous EDTA-Pb [53] and citrato-Pb [54] complexes.

leads to cation segregation at the micrometer scale and destroys the advantages of a gel-based process. For example, a Pb–Mg–Nb-EDTA gel formed with Pb:EDTA molar ratio of 1:4 forms a homogeneous gel which forms phase pure perovskite lead magnesium niobate on heating to 800°C. However, Pb_2EDTA_2 precipitates from a Pb–Mg–Nb-EDTA gel formed with Pb:EDTA mole ratio of 1:1 during dehydration. Consequently, after heating the phase separated gel to 800°C a significant amount of an intermediate pyrochlore phase (35 wt%) formed along with the desired perovskite phase (65 wt%).

The precipitation behavior of complexes of different carboxylate chelating agents are significantly different and is related to the extent of crosslinking between the carboxylato-metal complexes. The observation that precipitation is difficult to circumvent in EDTA gels compared to citrate gels is connected with the structure differences between citrato-metal and EDTA-metal complexes (Fig. 6). The EDTA ligand in the metal EDTA complex is typically seven-coordinated and all the functional groups are typically bonded to the metal cation. In citrato-metal complexes the alpha hydroxy ligand serves as a bridge between two metal centers, leading to planar complexes with uncomplexed carboxylate ligands [53,54]. The uncomplexed carboxylate groups in the citrato-metal complexes can form ionic bridges with metal centers of another complex. The metal carboxylate crosslinking reaction prevents precipitation of citrato-metal complexes in citrate gels. Consequently, citric acid is commonly used in the carboxylate gel process because citrato-metal complexes are stable to hydrolysis and ionically crosslink in a concentrated solution, thereby preventing precipitation during gelation. A high degree of crosslinking is also characteristic of the Pechini process where ethylene glycol is used as a solvent for citric acid and citrato-metal complexes. In an ethylene glycol medium, ester bonds form between the free carboxylate groups of citrato-metal complexes and alcohol groups of ethylene glycol [16,55]. The ester bonds crosslink carboxylato-metal complexes into low molecular weight oligomers and prevent precipitation. Moreover, the crosslinking reactions, viz. formation of ester bonds and ionic metal carboxylate bonds, also increase the viscosity of the solution. The increased viscosity lowers the diffusion rate of carboxylato-metal complexes and kinetically inhibits the phase separation process.

4. Gel thermolysis — alkoxides

After gel synthesis, typically the dried gel is heated to form a crystalline oxide or a dense oxide glass. During heating, gel structural evolution continues due to decomposition of organics and skeletal densification. Skeletal densification occurs by polymerization through continued condensation reactions and structural relaxation [8]. Structural relaxation occurs via diffusive movements of the gel network to the lower excess free volume of the gel and allows the structure to approach a configuration characteristic of a metastable liquid [8,56]. The processing stage wherein the low density skeletal structure of a dried gel is consolidated by heating to form a amorphous oxide is referred to as *thermolysis*. The structural rearrangements during thermolysis change the molecular arrangements in the gel as evidenced by changes in cation coordination [2,57]. Moreover, reactions with gases are also important during gel thermolysis. Gases are evolved due to condensation reactions or decomposition of organic ligand retained in the gel after hydrolysis. Consequently, the cation homogeneity of the gel prior to oxide formation is strongly affected by the thermal history of the sample. As will be discussed, thermolysis is shown to disrupt the homogeneity of some gels, such as lead-based perovskites and aluminosilicates while molecularly inhomogeneous systems, such as borosilicates and titania-silicates homogenize during thermolysis.

Alkoxide-derived mullite gels provide an excellent example of phase separation of a homo-

geneous gel during thermolysis. The homogeneity of aluminosilicate gels is strongly affected by the reaction of water vapor with the gel and structural rearrangements during skeletal densification. Huling and Messing [6] determined that partial pressure of water generated due to the condensation reactions during thermolysis has a significant effect on cation segregation in the aluminosilicates gel precursors to mullite and consequently mullite crystallization. Since the condensation rate is controlled by the rate of water or alcohol vapor diffusion through the gel, the effective vapor pressure in the gel depends on the pore size and pore volume in the gel [8]. Homogeneous gels with different pore structure and volume were prepared to study the effect of water vapor on the gel homogeneity during thermolysis. Aluminosilicate gel was prepared by the slow hydrolysis of $Al(NO_3)_3 \cdot 9H_2O$ and $Si(OEt)_4$ at 60°C. The gel was redispersed in excess ethanol, ethanol was evaporated and replaced with water to form a translucent sol. The sol was boiled at 100°C to form a transparent sol. The limpid sol was rapidly dried at 120°C to form a powder termed, a 'fresh gel'. The fresh gel powder was aged at 80°C in a humid atmosphere to form a clear sol, which was dried to form a transparent 'aged gel'. Aging the fresh gel in a condition of high solubility increases the pore size and pore volume and eliminates the gel microporosity. The fresh gel has a low surface area (2.5 m^2/g) indicating a microporous network not accessible to N_2. The aged gel has a surface area of 110 m^2/g indicating a mesoporous network. Since the water diffusion rate increases with an increase in pore size and pore volume, a lower vapor pressure is expected in the aged gels during thermolysis. Corresponding to the difference in the pore structure, there is also a significant difference in the crystallization behavior. On directly heating aged gels to 780°C, direct formation of o-mullite ($3Al_2O_3 \cdot 2SiO_2$) was observed. However, fresh gels were primarily amorphous with only traces of o-mullite at 780°C and formed t-mullite ($2Al_2O_3 \cdot SiO_2$) at 980°C. TEM observation of fresh gels heated to 900°C indicated that phase separation occurs in fresh gels leading to an interpenetrating structure of silica and alumina rich regions (Fig. 7). Due to the cation segregation in fresh gels at 900°C, t-mullite ($2Al_2O_3 \cdot SiO_2$) which is an

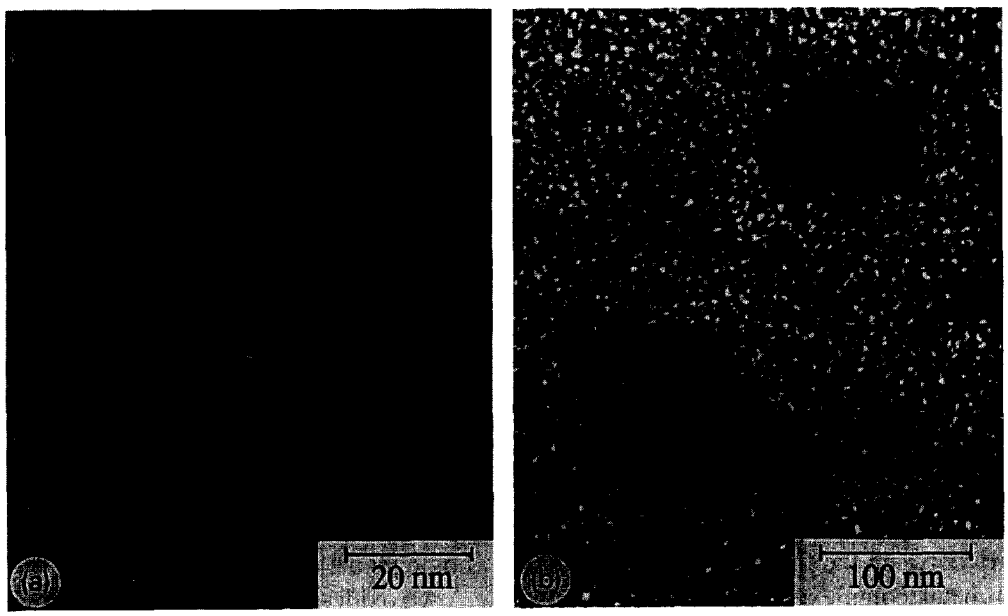

Fig. 7. TEM micrograph of fresh mullite gel heated to (a) 900°C for 2 h and (b) 1000°C for 2 h [6].

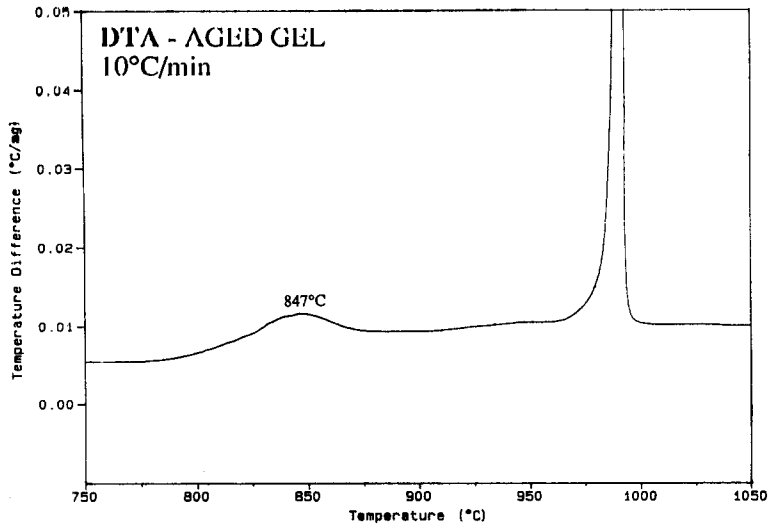

Fig. 8. DTA scans of an aged mullite gel heated at 10°C/min [6].

Al_2O_3-rich form of mullite crystallized at 980°C. A similar heterogeneous structure is also observed in phase separated glasses [58], which also crystallize into t-mullite ($2Al_2O_3 \cdot SiO_2$) on heating to 1000°C [59].

Due to the microporous nature of the fresh gel, the water vapor pressure is higher in the fresh gel which leads to rehydrolysis and cation segregation. The mesoporous structure of aged gels allows for faster removal of water and promotes direct o-mullite ($3Al_2O_3 \cdot 2SiO_2$) crystallization. The strong effect of water vapor on phase separation in mullite gels is due to the lower free energy of [AlO_6] compared to [AlO_4] species [13,60]. The presence of Al–O–Si bonds forces Al to assume a higher energy tetrahedral

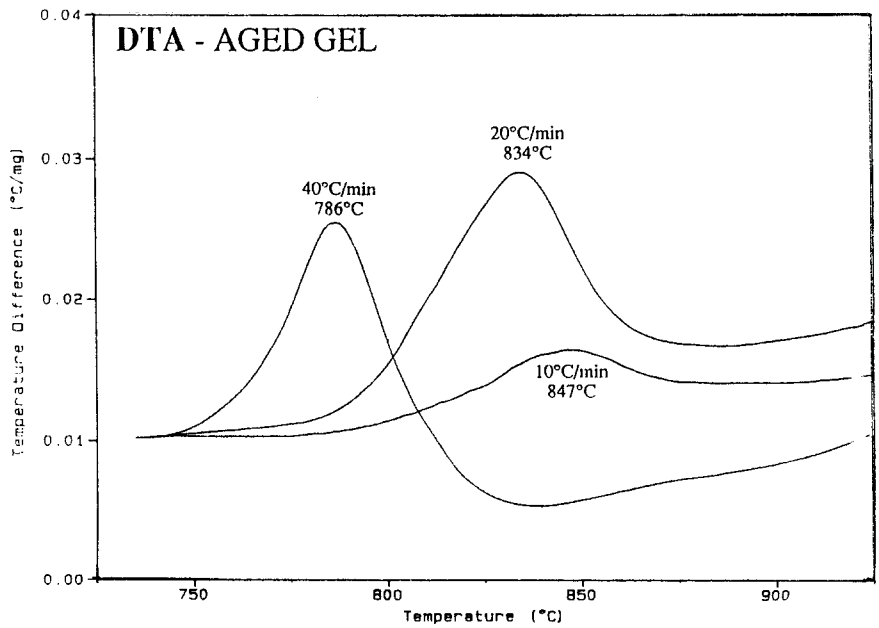

Fig. 9. DTA scans of an aged mullite gel heated at 10, 20 and 40°C/min [6].

position. Rehydrolysis of the Al–O–Si bond leads to the formation of [AlO_6] which is energetically favorable. An analogous process occurs during dealumination of zeolite in the presence of water [61]. Preferential hydrolysis of Al–O–Si bonds removes tetrahedrally-coordinated Al from the silicate network in the form of mobile Al species leading to cation segregation.

Because of the limiting effect of vapor diffusion on the condensation rate, the heating rate and gel size also strongly affect the structural changes during gel thermolysis [62]. Formation of o-mullite is also extremely sensitive to heating conditions [6,13]. A DTA scan of the aged gel heated at 10°C/min (Fig. 8) shows that very little o-mullite ($3Al_2O_3.2SiO_2$) forms on heating at 10°C/min (weak exotherm at 847°C) and most of the gel crystallizes to t-mullite ($2Al_2O_3 \cdot SiO_2$) (strong exotherm at 990°C). Faster heating rates (Fig. 9) enhanced o-mullite formation as evidenced by a lower temperature and an increase in the intensity of the exothermic peak for o-mullite crystallization. Hence, rapid heating and isothermal treatments to 780°C are most favorable for obtaining high yields of o-mullite. These results indicate that the mechanism of phase separation is similar for both fresh and aged gels. The separation phenomena is influenced by similar factors as involved in separation of aluminosilicate glasses upon cooling, i.e., driving force and atomic mobility. The driving force for chemical phase separation is the lowering of excess free energy when the components are allowed to rearrange and exist predominantly in their lowest free energy oxygen coordination-octahedral Al and tetrahedral Si. The skeletal densification due to condensation reactions and structural relaxation provides sufficient atomic mobility to cause cation segregation. Water plays the role of a mineralizer by breaking the Al–O–Si bonds [61] and weakening the gel network, thereby enhancing the rate of cation segregation. Hence, o-mullite formation is controlled by the relative rates of phase separation and o-mullite crystallization. During rapid heating cation segregation is circumvented and o-mullite crystallizes directly from the gel. However, during slow heating skeletal densification destroys the precursor homogeneity and results in t-mullite formation.

While reaction with water vapor and structural rearrangements due to skeletal densification lead to cation segregation in aluminosilicates, they improve gel homogeneity of lead zirconate titanate gels. Hirano et al. [63] studied the effect of water vapor treatment on crystallization of alkoxide derived lead zirconate titanate films. $Pb(OAc)_2$ was reacted with a refluxed mixture of $Zr(OEt)_4$ and $Ti(OEt)_4$ in ethanol, acetyl acetone was added to stabilize the solution and films were fabricated on substrates by spin coating. The films were dried and calcined in a mixture of water vapor and oxygen or pure O_2 and crystallized between 450 and 600°C. Water vapor treated films formed a highly oriented, phase pure perovskite layer on MgO (200) substrates at 600°C. However, in the absence of water vapor, perovskite crystallinity was poor and an intermediate pyrochlore phase formed at 600°C. Water vapor treatment removes residual alkoxy, acetate and carbonate generated during calcination, and organic pyrolysis is avoided which improves the quality of the film. Moreover, the condensation of hydroxylated species formed during water treatment increases the gel homogeneity and formation of phase pure perovskite.

Similarly skeletal densification is found to increase the homogeneity of several systems notably, borosilicates and titania silicates. Beier et al. [64] studied the structures of alkoxide-derived SiO_2–TiO_2–ZrO_2 gels using ^{29}Si-NMR and concluded that no Si–O–Ti or Si–O–Zr linkages were present in the dried gel. The absence of heterolinkages in the gel is expected due to the differences in the hydrolysis rates of Si and Ti or Zr alkoxides. Hayashi et al. [25] correlated the shrinkage behavior of SiO_2–TiO_2 gels with the homogeneity of the glasses formed by heating the gels. Gels prepared with low water concentration have a steady shrinkage

during thermolysis due to increased condensation reactions and a higher free volume associated with a poorly crosslinked structure. The weakly crosslinked gels completely densified into clear glasses during thermolysis. However, gels prepared with large amounts of water exhibited less skeletal densification and did not homogenize during thermolysis resulting in TiO_2 crystallization.

5. Gel thermolysis — carboxylates

The crosslinks in an alkoxide-derived gel are similar to metal oxides, namely metal oxygen bonds. Hence, the condensation of hydrolyzed metal centers is the primary reaction leading to polymerization of hydrolyzed alkoxides during all stages of processing viz. gelation, drying and thermolysis. Metal carboxylate gels are composed of carboxylato-metal complexes, crosslinked into a three dimensional structure with ionic metal-carboxyl and ammonium–carboxyl bonds or hydrogen bonds. Hence, during thermolysis there has to be a complete breakdown of the gel structure before oxide formation. Several reactions occur during thermolysis [19,65]; evaporation of water or solvents such as ethylene glycol, increase in polymerization due to ester formation between –C–OH and –COOH or between –C–OH and –C–OH groups, decomposition reactions of carboxylate complexes leading to formation of gases and an organic char, changes in the metal coordination sphere and nature of the metal-ligand bonding and possibly formation of *M*–O–*M* leading to formation of oligomers. In spite of the complexity of metal carboxylate decomposition, two basic stages of decomposition can be discerned.

The first stage involves scission of the ammonium–carboxylate bond, esters and hydrogen bonds in the amorphous gel at temperatures below 300°C [55,65]. The second stage involves the decomposition of the carboxylato-metal bonds within the carboxylate complex and the metal-carboxylate crosslinks which are bridging the different complexes. Oxide formation occurs with breakdown of the metal-carboxylate bond. Hence, in multication systems, cation homogeneity prior to oxide formation is controlled by the thermal stabilities of the metal-carboxylate bridges and the decomposition behavior of the different carboxylato-metal complexes. Typically the thermal stability of metal carboxylate bonds are different and carboxylato-metal complexes decompose at different temperatures, resulting in phase separation during gel thermolysis [50,66,67].

The best example of carboxylate gel phase separation is seen in the synthesis of cuprates such as $YBa_2Cu_3O_{7-x}$ [67]. A study of the individual citrate complexes indicates that Cu-citrate undergoes rapid decomposition at $<$ 250°C due to a strong catalytic effect of the Cu^+ to Cu^{2+} redox reaction on the oxidation of the citrate ligand [68]. However, Y-citrate and Ba-citrate have higher thermal stabilities and decompose to form Y_2O_3 and $BaCO_3$, respectively, between 400–500°C. The thermolysis behavior of the Y-citrate, Cu-citrate and Ba-citrate complexes are compared in Fig. 10. Consequently on heating a Y–Ba–Cu-citrate gels, Cu-citrate decomposes rapidly and phase separates to form Cu_2O or CuO. The formation of copper oxide(s) thus necessitates a high temperature solid state reaction ($>$ 900°C) to form $YBa_2Cu_3O_{7-x}$.

Another mechanism of phase separation is due to reaction with gaseous decomposition products during thermolysis. Unlike alkoxide-derived gels where the weight losses are usually $<$ 10 wt%, carboxylate gels lose up to 50% weight and evolve large amounts of gases; typically CO, CO_2 and H_2O. Gels containing electropositive metals such as alkali metals, alkaline earth metals [19,50] or lanthanides [69] react with carbon dioxide to form carbonates. Most carbonates, especially alkaline earth carbonates are stable up to 900°C, necessitating a high temperature calcination for cation homogenization. Hence, it is important to avoid the forma-

tion of carbonates during gel decomposition. Zhang et al. studied Y–Ba–Cu–O crystallization from a Y–Ba–Cu-citrate precursor prepared in ethylene glycol [19]. On heating the gel in air or O_2 at 775°C, Ba reacts with the evolved carbon dioxide and forms $BaCO_3$. On heating the precursor in a mild vacuum (10^{-2} PO_2), 98% of the total weight loss is observed at 400°C and formation of $BaCO_3$ was circumvented. The XRD patterns of the Y–Ba–Cu-citrate precursor heated to 775°C in air, O_2 and 10^{-2} atm PO_2 are compared in Fig. 11 [19]. IR spectra of powder calcined at 775°C in vacuum, confirmed the absence of carbonates. Nearly phase pure $YBa_2Cu_3O_{7-x}$ forms at 830°C, with minor amounts of $BaCuO_2$ and $Cu_2Y_2O_5$, in the absence of $BaCO_3$. Thus, gel homogeneity of carboxylate gels is strongly affected by reactions during gel thermolysis.

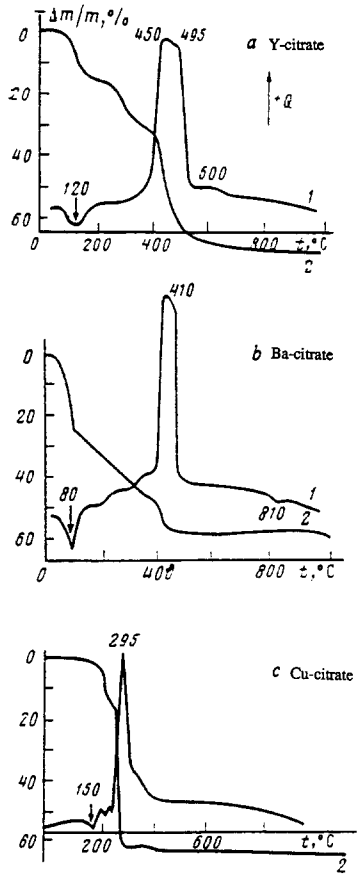

Fig. 10. DTA (plot #1) and TGA (plot #2) scans of the (a) Y-citrate, (b) Ba-citrate and (c) Cu-citrate complexes heated at 2.5°C/min in air [67], showing the difference in the decomposition temperatures of the Y-, Ba- and Cu-citrate complexes.

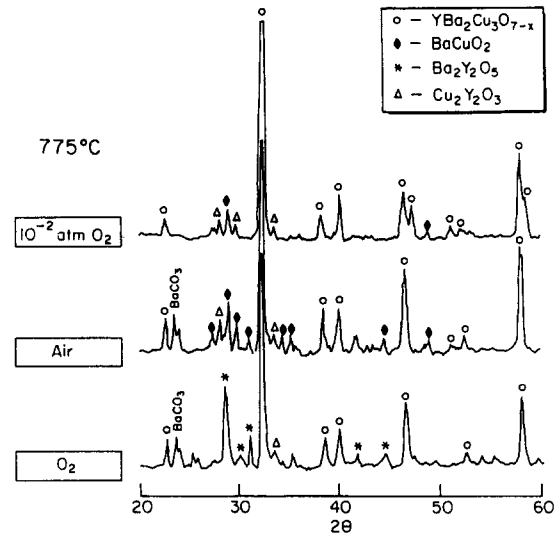

Fig. 11. XRD patterns of the Y–Ba–Cu-citrate precursor heated to 775°C for 1 h in air, O_2 and 10^{-2} atm O_2 [19], illustrating that $BaCO_3$ formation can be prevented by heating the precursor in a mild vacuum.

6. Oxide crystallization

In spite of a homogeneous cation distribution in the gel after gel thermolysis, phase separation is observed during oxide formation in a variety of systems [15,22]. The phenomenon of oxide crystallization is well studied in the glass-ceramics literature. There are several factors which are known to influence crystallization which include: the presence of dissolved impurities, gel surface area and the presence of minor amounts of second phases [70]. The presence of dissolved impurities, especially OH^- is found to lower the viscosity of silicate gels and enhance the oxide crystallization kinetics in several different gel systems. Moreover, in the Al_2O_3–ZrO_2–SiO_2–Na_2O system, the concentration of OH^- also alters the crystallization pathway of the gels [71]. Similarly, the presence of small amounts of second phase impurities in

an otherwise homogeneous gel drastically affects crystallization [70,72], due to the high interfacial area between the two phases. Huling and Messing [72] studied the effect of adding colloidal alumina and silica to a homogeneous mullite gel prepared by slow hydrolysis of $Al(NO_3)_3 \cdot 9H_2O$ and $Si(OEt)_4$. The gel crystallized into t-mullite ($2Al_2O_3 \cdot SiO_2$) on heating to 1000°C in the absence of second phase additions. However, as low as 10 wt% additions of second phases leads to phase separation in the matrix with the crystallization of a spinel ($6Al_2O_3 \cdot SiO_2$) along with t-mullite ($2Al_2O_3 \cdot SiO_2$).

The difference in the crystallization behavior of different gels and the influence of processing and impurities on crystallization can be understood from nucleation theory. Nucleation is the formation of the smallest stable particle of a crystalline phase in the amorphous gel matrix. Hence, the phase and stoichiometry of the oxide is determined by the nucleation conditions. The classical steady state homogeneous nucleation rate [7] is given by J_s^*,

$$J_s^* = z\beta N \exp\left(\frac{-\Delta G^*_{\text{hom}}}{kT}\right)$$

where z is the Zeldovich factor, β is the rate of single atoms joining a cluster, N is the number of nucleation sites per unit volume (for homogeneous nucleation N = the number of atoms per unit volume), T is the temperature, k is the Boltzmann constant and ΔG^*_{hom} is the activation energy for homogeneous nucleation.

$$\Delta G^*_{hom} = \frac{16\pi\gamma^3_{\alpha\beta}}{3(\Delta G_v + \Delta G_\epsilon)^2}$$

where ΔG_v is the thermodynamic driving force for crystallization, ΔG_ϵ is the strain energy associated with the transformation and $\gamma_{\alpha\beta}$ is the surface energy of the nucleus–gel interface.

In general, the activation energy for homogeneous nucleation is high due to a high nucleus–matrix surface energy. Consequently, nucleation from gels is usually observed at heterogeneous sites such as interfaces or surface heterogeneities. Heterogeneities replace part of the high energy nucleus–gel interface with a lower energy heterogeneity-nucleus interface, thus, lowering the overall activation barrier. The activation barrier during heterogeneous barrier is given by,

$\Delta G^*_{\text{het}} = \Delta G^*_{\text{hom}} f(\phi)$, where $f(\phi)$ is a geometric factor which depends on the surface energies of the substrate, gel and nucleus [73]. The number of nucleation sites in heterogeneous nucleation is limited by the number of heterogeneities per unit volume, N_{het}. For heterogeneous nucleation to be favored over homogeneous nucleation, $f(\phi)$ must be much smaller than unity. During crystallization the phase with the highest nucleation rate controls phase formation. The criteria for a high nucleation rate are a high negative free energy of formation (ΔG_v), a low strain energy (ΔG_ϵ), a low nucleus to matrix interfacial energy ($\gamma_{\alpha\beta}$) and a large heterogeneous nucleation site density (N_{het}). Based only on the free energy of formation, the equilibrium phase has the most $-\Delta G_v$ and the maximum driving force. However, strain energy differences, surface energy and nucleation site density also affect the nucleation rate and such kinetic factors can lead to the nucleation of non-equilibrium phases.

The effect of kinetic factors explains the crystallization of non-equilibrium phases from melt-formed glasses or sintered gels in contrast to crystallization of equilibrium phases from gels [70]. Gels have a large excess free energy due to an open structure with an excess free volume much higher than glasses or supercooled liquids [74], a high concentration of high energy sites which can act as potential heterogeneous sites [56] and a lower viscosity due to a higher concentration of internal hydroxyl groups [8]. Moreover, strain energy is expected to be insignificant in gels with open structures compared to dense glasses. Hence, there is a large driving force for the formation of the phase with the lowest free energy in gels, resulting in crystallization of equilibrium phases. However, in

glasses kinetic factors can dominate leading to phase separation during crystallization.

The factors that influence the nucleation rate can be classified as either intrinsic or extrinsic. Some factors are intrinsic to the equilibrium and competing metastable phases such as the respective free energies of formation, crystal density, surface energy or compositional stability range. Extrinsic factors are usually processing related, such as stoichiometry of heterometallic complexes, heating rate during oxide crystallization, presence of dissolved impurities or second phase impurities [70,72]. The best illustration of intrinsic effects is seen for crystallization of glass ceramic compositions from gel-derived glasses. Typically, the phase with the structure closest to the glass has the highest nucleation site density and is the first phase to crystallize from gels. A high nucleation site density explains the formation of a metastable phase with the β-quartz structure (μ-cordierite and β-eucryptite) before formation of the stable α-cordierite in $MgO–Al_2O_3–SiO_2$ gels [15,75] or β-spodumene $Li_2O–Al_2O_3–SiO_2$ gels [76]. Consequently, in spite of a larger ΔG_v for α-cordierite, μ-cordierite forms from the gel due to a higher nucleation site density. Mathematically,

$$N_\mu \exp\left(\frac{-\Delta G_\mu^*}{kT}\right) > N_\alpha \exp\left(\frac{-\Delta G_\alpha^*}{kT}\right)$$

where N_μ and N_α are the heterogeneous nucleation site densities and ΔG_μ^* and ΔG_α^* are the heterogeneous nucleation barriers for μ-cordierite and α-cordierite, respectively.

The phase separation of μ-cordierite can be circumvented by the addition of fine particles of α-cordierite (seeding) to gels [75]. α-cordierite seed particles serve as epitaxial sites for α-cordierite nucleation, which increases its heterogeneous nucleation site density (N_α) and drastically lowers the activation energy for α-cordierite formation (ΔG_α^*) at these sites [73,77]. Hence, on α-cordierite addition,

$$\Delta G_\mu^* \ll \Delta G_\alpha^*$$

and

$$N_\mu \exp\left(\frac{-\Delta G_\mu^*}{kT}\right) < N_\alpha \exp\left(\frac{-\Delta G_\alpha^*}{kT}\right)$$

thereby resulting in direct α-cordierite crystallization from the amorphous matrix. Apart from cordierite, seeding has also been used in several multicomponent systems to avoid phase separation during crystallization [77].

Apart from glass ceramics, differences in heterogeneous site density are also responsible for the formation of intermediates with a large compositional stability or for the formation of disordered intermediates before formation of ordered phases. The best examples are seen in the literature of lead-based perovskites where an intermediate pyrochlore phase is typically reported

Fig. 12. Bright field TEM micrograph of perovskite rosettes growing from a fine-grained pyrochlore matrix in an alkoxide-derived lead zirconate titanate thin film heated to 650°C [80]. Insets are selected area diffraction patterns taken along the [111] zone axis in a single perovskite rosette (left) and from the polycrystalline pyrochlore matrix (right).

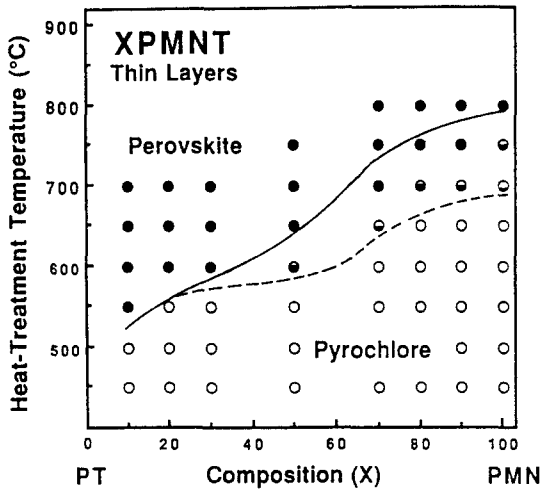

Fig. 13. Temperature regimes for pyrochlore and perovskite formation in PMN–PT thin layers [82].

before formation of the stable perovskite phase. Pyrochlore crystallization is an intrinsic effect as it forms from all precursor systems viz. alkoxide-derived gels [78], carboxylates [22], co-precipitated hydroxides [79], or oxalates and mixtures of oxides or carbonates [80]. The perovskite phase is the most stable structure with the highest negative ΔG_v. With the density and surface differences between the perovskite and pyrochlore phases not expected to be significant, the activation energy for the perovskite phase can be expected to be lower than that for the pyrochlore. Hence, crystallization of pyrochlore indicates a higher pyrochlore nucleation site density compared to the perovskite. The pyrochlore nucleation density (N_{py}) and perovskite nucleation site density (N_{pe}) can be estimated from the grain sizes of the respective phases after crystallization [81]. A high pyrochlore nucleation density is supported by the observation that the pyrochlore grain size is extremely small (10–15 nm) compared to the perovskite phase (0.5–3 μm) (Fig. 12). Pyrochlore's higher nucleation site density is related to its disordered structure and structural stability over a large compositional range. Pyrochlore in the Pb–Nb–O system are reported with stoichiometries ranging from *A*-deficient $A_{1.5}B_2O_{9.75}$ to stoichiometric $A_2B_2O_7$ to *B*-deficient $A_2B_{1.6}O_6$ and $A_2B_{1.33}O_{5.33}$ compositions [82]. However, the perovskite composition

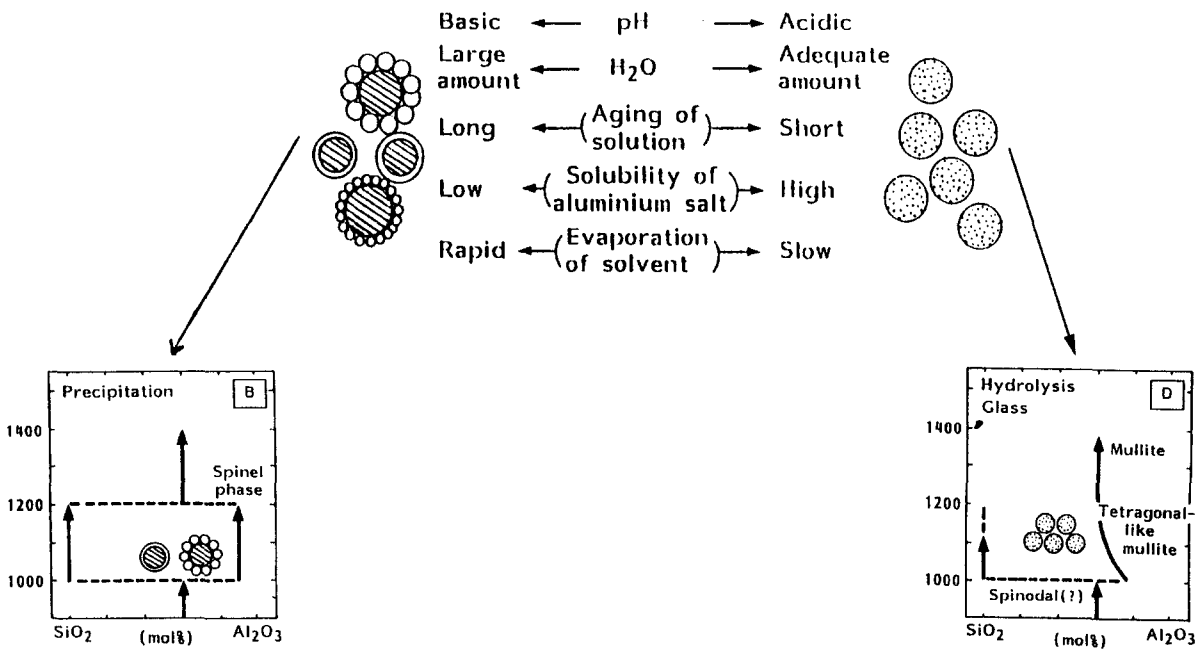

Fig. 14. Schematic of the effects of processing variables on homogeneity of mullite gels and mullite crystallization [1].

is fixed at $A:B$ stoichiometry of 1:1, with a deviation of < 1 mol%. Consequently, the probability of statistical fluctuations leading to a composition closer to the pyrochlore structure is much greater than the perovskite structure. Mathematically, $N_{pe} \ll N_{py}$. Hence, the nucleation rate of pyrochlore (J^*_{pe}) is much greater than the perovskite nucleation rate (J^*_{pe}) and the pyrochlore forms first during gel crystallization on slow heating and/or annealing at low temperatures (400–500°C).

On direct annealing at high temperatures, ca. 600–700°C for PZT [4] and ca. 750–800°C for lead magnesium niobate (PMN) gels [83], the perovskite phase forms directly from the gel. The effect of annealing temperature and composition on perovskite phase formation in PMN is summarized in Fig. 13 [82]. The strong influence of heating rate and annealing temperature is an excellent example of extrinsic factors, such as the addition of seeds, which affect oxide crystallization. The influence of crystallization temperature on phase formation can also be rationalized from nucleation theory. Perovskite is the stable phase and its free energy of formation (ΔG_v^{pe}) is more negative than free energy of formation of pyrochlore (ΔG_v^{py}) viz. $\Delta G_v^{py} < \Delta G_v^{pe}$. Hence, the activation energy barrier for heterogeneous nucleation of perovskite (ΔG^*_{pe}) is lower than that for the pyrochlore (ΔG^*_{py}), viz. $\Delta G^*_{py} < \Delta G^*_{pe}$. However, $(N\beta)_{pe} \ll (N\beta)_{py}$ and at low temperatures $J^*_{py} \gg J^*_{pe}$. As the crystallization temperature increases, the effect of the activation energy is very important due to the exponential dependence of nucleation rate to activation energy. Above a critical temperature,

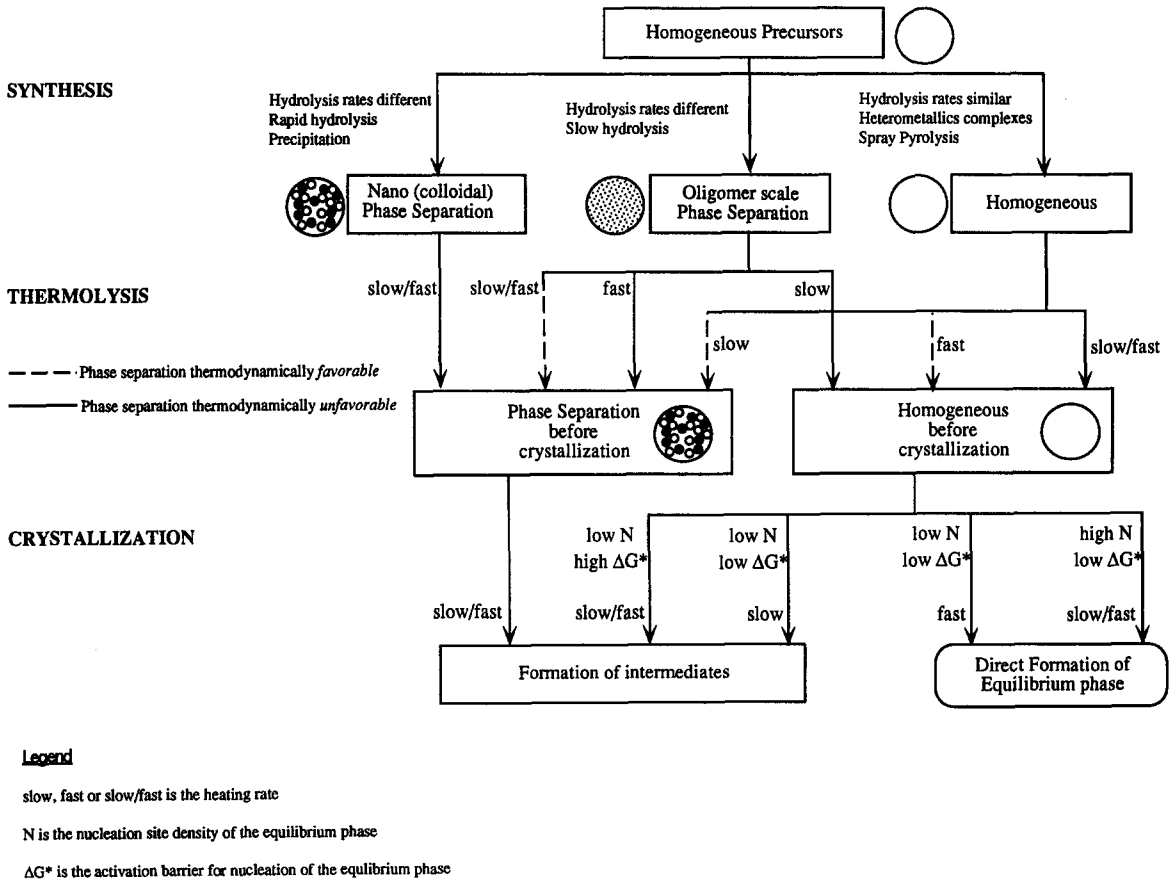

Fig. 15. Phase separation mechanisms in gel-derived multicomponent oxides.

$N_{py}\exp(-\Delta G^*_{py}/kT) < N_{pe}\exp(-\Delta G^*_{pe}/kT)$ and perovskite nucleation is favored.

7. Conclusions

The direct crystallization of an equilibrium oxide phase from gels is determined by cation homogeneity in the precursor prior to oxide crystallization and the nucleation rates of competing crystalline intermediate oxides. Phase separation during gel synthesis is primarily due to differences in the hydrolysis rates of alkoxides in alkoxide-derived gels and selective precipitation of cations in the carboxylate gels. On heating alkoxide-derived gels, structural rearrangement associated with skeletal densification can lead to homogenization or phase separation depending upon the thermodynamic driving force. In carboxylate gels differences in the decomposition temperatures of the carboxylatometal complexes can result in phase separation. Reactions with gases can cause phase separation in both carboxylate and alkoxide gels. Phase separation during oxide crystallization is related to differences in nucleation rates between the competing oxides and is influenced primarily by the density of heterogeneous sites and the free energy barrier to nucleation.

Based on the oxide crystallization behavior of different gel systems presented in this paper, it is apparent that phase separation is strongly influenced by the processing conditions. The effect of processing variables on cation homogeneity and oxide phase development is shown schematically for in Fig. 14 for mullite gels [1]. The discussion on mullite gels illustrates that intrinsic factors causing chemical phase separation can be overcome by controlling the processing conditions during all three stages, viz. synthesis, thermolysis and crystallization. The combined role of different phase separation mechanisms and processing conditions on oxide crystallization pathway is illustrated in Fig. 15.

References

[1] K. Okada, N. Otsuka and S. Somiya, Ceram. Bull. 70 (1991) 1633.
[2] U. Selvaraj, S. Komarneni and R. Roy, J. Am. Ceram. Soc. 73 (1990) 3663.
[3] J.-H. Choy, J.-S. Yoo, et al., Mater. Res. Bull. 25 (1990) 283.
[4] C.D.E. Lakeman and D.A. Payne, J. Am. Ceram. Soc. 75 (1992) 3091.
[5] C.-C. Hsueh and M.L. Mecartney, J. Mater. Res. 6 (1991) 2208.
[6] J.C. Huling and G.L. Messing, J. Non-Cryst. Solids 147 and 148 (1992) 213.
[7] D.A. Porter and K.E. Easterling, Phase Transformations in Metals and Alloys, 2nd Ed. (Chapman and Hall, London, 1992).
[8] C.J. Brinker and G.W. Scherer, Sol-Gel Science (Academic Press, San Diego, CA 1990).
[9] D.R. Paul and S. Newman, eds., Polymer Blends, Vol. 1 (Academic Press, San Diego, CA, 1978).
[10] F.F. Lange, M.L. Balmer and C.G. Levi, J. Sol-Gel Sci. Technol. 2 (1994) 317.
[11] T. Hayashi and H. Saito, J. Mater. Sci. 15 (1980) 1765.
[12] M. Yamane and T. Kojima, J. Non-Cryst. Solids 44 (1981) 181.
[13] J.C. Huling, Controlled Crystallization of Sol-Gel Mullite, Ph.D. Thesis, The Pennsylvania State University, 1992.
[14] H. Schneider, K. Okada and J.A. Pask, Mullite and Mullite Ceramics (Wiley, Chichester, UK, 1994).
[15] M. Okuyama, T. Fukui and C. Sakurai, J. Am. Ceram. Soc. 75 (1992) 153.
[16] M.P. Pechini, US Patent No. 3330697, July 11, 1967.
[17] S. Kumar, G.L. Messing and W.B. White, J. Am. Ceram. Soc. 76 (1993) 617.
[18] P.S. Devi and M.S. Rao, Mater. Lett. 16 (1993) 14.
[19] S.C. Zhang, G.L. Messing, et al., J. Mater. Res. 5 (1990) 1806.
[20] A. Aiko, S. Ohno and Y. Muramatsu, J. Non-Cryst. Solids 147 and 148 (1992) 720.
[21] M.A. Zaghete, C.O.P. Santos, et al., J. Am. Ceram. Soc. 75 (1992) 2088.
[22] H.U. Anderson, M.J. Pennell and J.P. Guha, Adv. Ceram. 21 (1987) 91.
[23] J-P. Boilot, F. Chaput and J.C. Pouxviel, Silicates Ind. 11–12 (1989) 187.
[24] J. Livage, M. Henry and C. Sanchez, Progr. in Solid State Chem. 18 (1988) 259.
[25] T. Hayashi, T. Yamada and H. Saito, J. Mater. Sci. 18 (1983) 3137.
[26] B.E. Yoldas and D.P. Partlow, J. Mater. Sci. 23 (1988) 1895.
[27] S. Sen and S. Thiagarajan, Ceram. Int. 14 (1988) 77.
[28] S. Mitachi, M. Matsuzawa, et al., Ceram. Trans. 6 (1990) 275.
[29] K. Okada and N. Otsuka, J. Am. Ceram. Soc. 69 (1986) 652.
[30] J. Sanz, I. Sobrados, et al., J. Am. Ceram. Soc. 74 (1991) 2398.

[31] M. Okuyama, T. Fukui and C. Sakurai, J. Non-Cryst. Solids 144 (1992) 298.
[32] K. Jones, T. Davies, et al., In: eds. C.J. Brinker, D.E. Clark and D.R. Uhlrich, Mater. Res. Soc. Symp. Proc. 73 (1986) 111, Materials Research Society, Pittsburgh, PA.
[33] K.G. Caulton and L.G. Hubert-Pfalzgraf, Chem. Rev. 90 (1990) 969.
[34] R.C. Mehrotra, J. Sol-Gel Sci. Technol. 2 (1994) 1.
[35] J.C. Pouxiel, J.P. Boilot, et al., Mater. Res. Soc. Symp. Proc. 73 (1986) 269.
[36] K. Kezuka, Y. Hayashi and T. Yamaguchi, J. Am. Ceram. Soc. 72 (1989) 1660.
[37] S. Hirano and K. Kato, Adv. Ceram. Mater. 2 (1987) 142.
[38] O. Sakurai, N. Mizutani and M. Kato, J. Ceram. Soc. Jpn. (Intl. Ed.) 96 (1988) 628.
[39] H. Suzuki and H. Saito, J. Ceram. Soc. Jpn. (Intl. Ed.) 95 (1987) 654.
[40] S. Kanzaki, S. Prochazka, et al., J. Am. Ceram. Soc. 68 (1985) C6.
[41] C.F. Baes and R.E. Mesmer, The Hydrolysis of Metal Cations (Wiley, New York, 1976).
[42] A.C. Pierre, T. Nickerson and W. Kresic, J. Non-Crystall. Solids 121 (1990) 45.
[43] J. Yang, W. Weng and Z. Ding, J. Sol-Gel Sci. Technol. 4 (1995) 187.
[44] J. Livage, J. Henry, J.P. Jolivet and C. Sanchez, J. Mater. Education 13 (1991) 233.
[45] W.J. MacKnight and T.R. Earnest, Jr., J. Polym. Sci. Macromol. Rev. 16 (1981) 41.
[46] J. Economy, J.H. Mason and L.C. Wohrer, J. Polym. Sci. Part A-1 8 (1970) 2231.
[47] E.N. Baker, H.M. Baker, et al., Inorg. Chim. Acta 78 (1983) 281.
[48] C-T. Chu and B. Dunn, J. Am. Ceram. Soc. 70 (1987) C-375.
[49] K.N. Pearce, Aus. J. Chem. 33 (1980) 1511.
[50] P. Karen and A. Kjekshus, J. Am. Ceram. Soc. 77 (1994) 547.
[51] L-G. Ekstrom and A. Olin, Chem. Scripta, 13 (1978–1979) 10.
[52] M. Bobtelsky and B. Graus, J. Am. Chem. Soc. 75 (1953) 4172.
[53] P.G. Harrison and A.T. Steel, J. Organometall. Chem. 239 (1982) 105.
[54] A.J. Francis, C.J. Dodge and J.B. Gillow, Nature (London) 356 (1992) 140.
[55] S.G. Cho, P.F. Johnson and R.A. Condrate, Sr., J. Mater. Sci. 25 (1990) 4738.
[56] F. Orgaz-Orgaz, J. Non-Cryst. Solids 100 (1988) 115.
[57] A.D. Irwin, J.S. Holmgren and J. Jonas, J. Non-Cryst. Solids, 101 (1988) 249.
[58] J.F. MacDowell and G.H. Beall, J. Am. Ceram. Soc. 52 (1969) 17.
[59] A. Yasumori, M. Iwasaki, et al., Phys. Chem. Glasses 31 (1990) 1.
[60] H. Morikawa, S. Miwa, et al., J. Am. Ceram. Soc. 65 (1982) 78.
[61] G.T. Kerr, J. Phys. Chem. 71 (1967) 4155.
[62] B.E. Yoldas, J. Sol-Gel Sci. Technol. 1 (1993) 65.
[63] S. Hirano, T. Yogo, et al., J. Am. Ceram. Soc. 75 (1992) 2785.
[64] W. Beier, A.A. Goktas and G.H. Frischat, J. Non-Cryst. Solids 121 (1990) 163.
[65] P.G. Desai, Z. Xu and J.A. Lewis, J. Am. Ceram. Soc. 78 (1995) 2881.
[66] S-Y. Chen and I-W. Chen, J. Am. Ceram. Soc. 77 (1994) 2332.
[67] S.P. Tolochko, I.F. Kononyuk, et al., Russian J. Inorg. Chem. 36 (1991) 275.
[68] PH. Courty, H. Ajot, et al., Powder Technol. 7 (1973) 21.
[69] P.S. Devi and M.S. Rao, Thermochim. Acta 15 (1989) 181.
[70] D.R. Uhlmann, M.C. Weinberg and G. Teowee, J. Non-Cryst. Solids 100 (1988) 154.
[71] I.M. Low and R. McPherson, J. Mater. Sci. 23 (1988) 3544.
[72] J.C. Huling and G.L. Messing, J. Am. Ceram. Soc. 74 (1991) 2374.
[73] J.L. McArdle and G.L. Messing, Adv. Ceram. Mater. 3 (1988) 387.
[74] R. Roy, J. Am. Ceram. Soc. 56 (1969) 344.
[75] M. Okuyama, T. Fukui and C. Sakurai, J. Mater. Res. 7 (1992) 2281.
[76] G.S. Lee, G.L. Messing and F.G.A. Delaat, J. Non-Cryst. Solids 116 (1990) 125.
[77] G. Vilmin, S. Komarneni and R. Roy, J. Mater. Res. 2 (1987) 489.
[78] F. Chaput, J.-P. Boilot, et al., J. Am. Ceram. Soc. 72 (1989) 1335.
[79] T. Ando, R. Suyama and K. Tanemoto, Jpn. J. Appl. Phys. 30 (1991) 775.
[80] S.L. Swartz and T.R. Shrout, Mater. Res. Soc. Bull. 17 (1982) 1245.
[81] A.H. Carim, B.A. Tuttle, et al., J. Am. Ceram. Soc. 74 (1991) 1455.
[82] M. Dambekalne, I. Brante and A. Sternberg, Ferroelectrics 90 (1989) 1.
[83] L.F. Francis and D.A. Payne, J. Am. Ceram. Soc. 74 (1991) 3000.